ISSN 1070-3632, Russian Journal of General Chemistry, 2013, Vol. 83, No. 6, pp. 1021–1028. © Pleiades Publishing, Ltd., 2013.
Original Russian Text © N.I. Skripov, T.P. Stepanova, L.B. Belykh, F.K. Schmidt, 2013, published in Zhurnal Obshchei Khimii, 2013, Vol. 83, No. 6, pp. 889–896.

The Nature of Nanoparticles Formed in the System $PdCl_2$–Elemental Phosphorus

N. I. Skripov, T. P. Stepanova, L. B. Belykh, and **F. K. Schmidt**

Irkutsk State University, ul. K. Marksa 1, Irkutsk, 664003 Russia
e-mail: belykh@chem.isu.ru

Received April 12, 2012

Abstract—The state of palladium in nanoparticles formed in the system $PdCl_2$ – elemental phosphorus in an inert atmosphere was identified using X-ray diffraction (XRD), high-resolution transmission electron microscopy (HRTEM), X-ray photoelectron spectroscopy (XPS). Palladium phosphides of different composition and Pd(0) clusters are shown to form as a result of a redox process. According to the XPS data, the structures of nanoparticles are of the core-shell type. The interaction of $PdCl_2$ with P_4 is followed not only by the hydrolysis of the solvent (DMF) accelerated by hydrochloric acid, but also by the decomposition catalyzed by palladium cluster of organic compounds. The formed graphite and phosphoric acids stabilize the nanoparticles.

DOI: 10.1134/S1070363213060029

The interest to the studies of the nature and physicochemical properties of nanoclusters, nanostructures and nanomaterials, including nanodimensional catalysts based on the transition metals has grown sharply in the last two decades [1–6]. This is due to the size quantization effect in nanoparticles, which drastically changes many properties of nanosystems, including catalytic properties, and opens new possibilities for creation of new and modification of existing catalysts for definite processes.

Liquid phase formation of metal nanoclusters by the method of chemical condensation is often followed by the processes of decomposition of the reducer [1, 7], solvent [4, 8], and stabilizing ligands [9] catalyzed by these clusters. This leads to modification of nanoparticles and, as a result, to variation in their chemical properties, which may be one of the reasons of contradictory literature data on the catalytic properties of the metal nanoclusters.

Earlier we have shown that not only phosphines [9] but elemental phosphorus itself [10] has a strong promoting effect on the properties of palladium catalysts in hydrogenation of unsaturated compounds, nitro and carbonyl groups under mild conditions. The modifying effect of phosphorus depends on the nature of the acidoligand in the precursor, the reducer, the ratio P/Pd, and concentration of the catalyst. In the case of oxygen-containing precursors the introduction of elemental phosphorus into the reaction system in small amounts (P/Pd < 0.7) prior to the stage of reduction of PdX_2 (X = acac, OAc) with hydrogen has a promoting effect on the properties of the palladium catalyst, substantially increasing the turn-over frequency (TOF) and turn-over number (TON) [10]. When forming the catalyst on the basis of $PdCl_2$ [8] or $Pd(dba)_2$ [dba is bis(dibenzylideneacetone)] [11] the introduction of elemental phosphorus increases only the productivity of the catalyst whereas its activity decreases with the increase of phosphorus concentration.

To establish the regularities of the formation of the palladium catalyst of hydrogenation we have performed investigation of the products of the reaction between $PdCl_2$ and elemental phosphorus in an inert atmosphere using the methods of X-ray diffraction (XRD), high-resolution transmission electron microscopy (HRTEM), X-ray photoelectron spectroscopy (XPS).

Earlier we have shown that the redox reaction of $PdCl_2$ and elemental phosphorus in an inert atmosphere in DMF proceeds with a high rate under mild conditions [8]. The conversion of $PdCl_2$ measured by the potentiometric titration of the concentration of

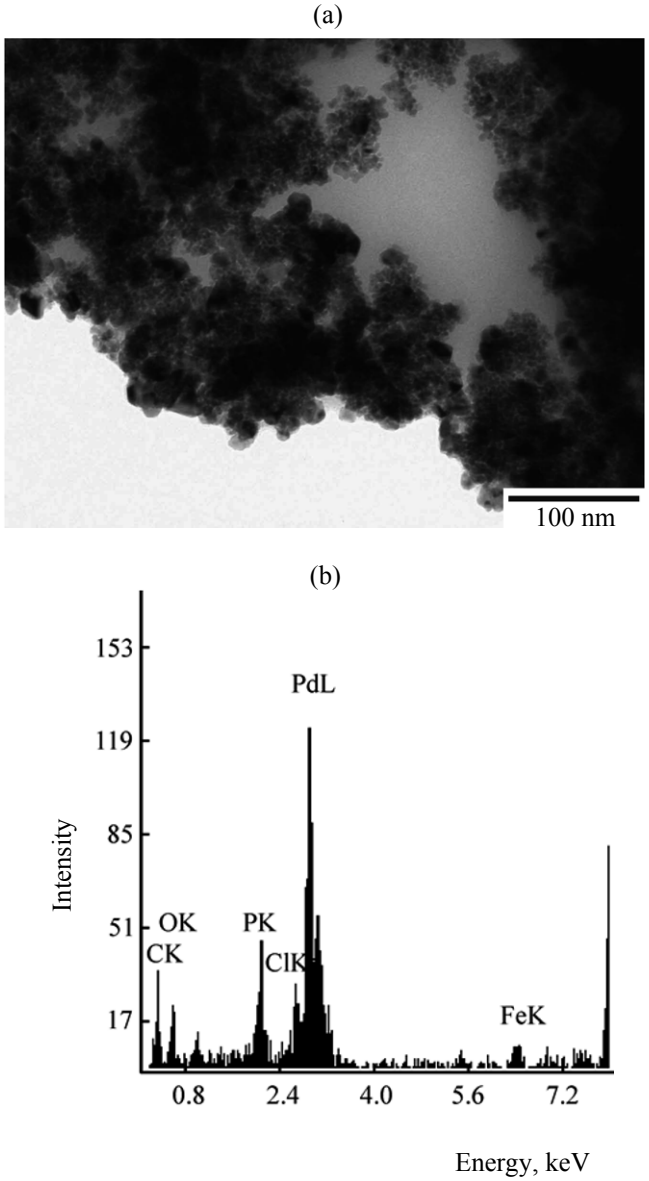

Fig. 1. TEM image and EDXS spectrum of the sample isolated from the system $PdCl_2$–0.3 P in DMF.

the formed hydrochloric acid varies from 34% at P/Pd = 0.3 to 84% when the ratio P/Pd increases to 1.0. In spite of nonquantitative conversion of $PdCl_2$ at the ratio P/Pd < 1, we have studied the products of the reaction of $PdCl_2$ with elemental phosphorus in argon at [P]/[Pd] = 0.3 which was further used for the formation of the hydrogenation catalysts.

In the ^{31}P NMR spectrum of the system $PdCl_2$–0.3P the signal of white phosphorus (δ_P = –520 ppm) disappeared already after 5 min from the beginning of the reaction, and the signals corresponding to phosphorous (δ_P = 4.4 ppm, J_{P-H} = 640 Hz) and phosphoric acids (δ_P = 3.4 ppm) were detected. The black precipitate isolated from the reaction mixture is X-ray amorphous. On the diffraction curve the reflexes of crystalline phase belonging to unreacted $PdCl_2$ and a diffuse halo in the range of angles of reflection 2θ = 35°–45° were detected. In this range the most intensive diffraction maxima of palladium metal and palladium phosphides appear [12]. The coherent scattering area (CSA) calculated from the Selyakov-Sherrer formula was 3.7 nm. After the sample was converted into the crystalline state, palladium phosphides Pd_6P, Pd_5P_2 and Pd_3P, as well as NH_4Cl were identified in it using XRD method. The formation of NH_4Cl is the result of hydrolysis of DMF accelerated by the formed hydrochloric acid, and of the thermal destruction of dimethylammonium chloride [8].

$$HC(O)N(CH_3)_2 + H_2O \xrightarrow{HCl} HCOOH + NH(CH_3)_2,$$

$$HN(CH_3)_2 + HCl = [NH_2(CH_3)_2]Cl,$$

$$HN(CH_3)_2 + HCl \xrightarrow{200–300°C} NH_2CH_3 + CH_3Cl,$$

$$NH_2CH_3 + HCl \xrightarrow{200–300°C} NH_3 + CH_3Cl,$$

$$NH_3 + HCl = [NH_4]Cl.$$

Since palladium phosphides Pd_5P_2, Pd_3P, Pd_6P were identified in the sample after it was subjected to the temperature control, the question arises if they were not formed due to solid phase transformations of palladium compounds at high temperature during the conversion of the sample into the crystalline state.

It is well known that if the size of crystallites is less than 100 nm, the reflexes of the crystalline phase on the diffraction curve broaden, and when the CSA of the size of ca. 3 nm is reached they become so broad that the compound cannot be identified by XRD method. At the same time, the HRTEM method allows to identify crystalline structure even for nanoparticles of 1 nm size and to determine the lattice parameter which is used for identification of the phase of the compound. Therefore, we have additionally studied the structure of the sample and determined its elemental composition by the HRTEM method. The overall view of the sample and its energy dispersive X-ray spectrum (EDXS) spectrum are shown in Fig. 1.

From the EDXS data, the ratio Pd/P in the sample is ca. 3:1. Analysis at different points of the surface of

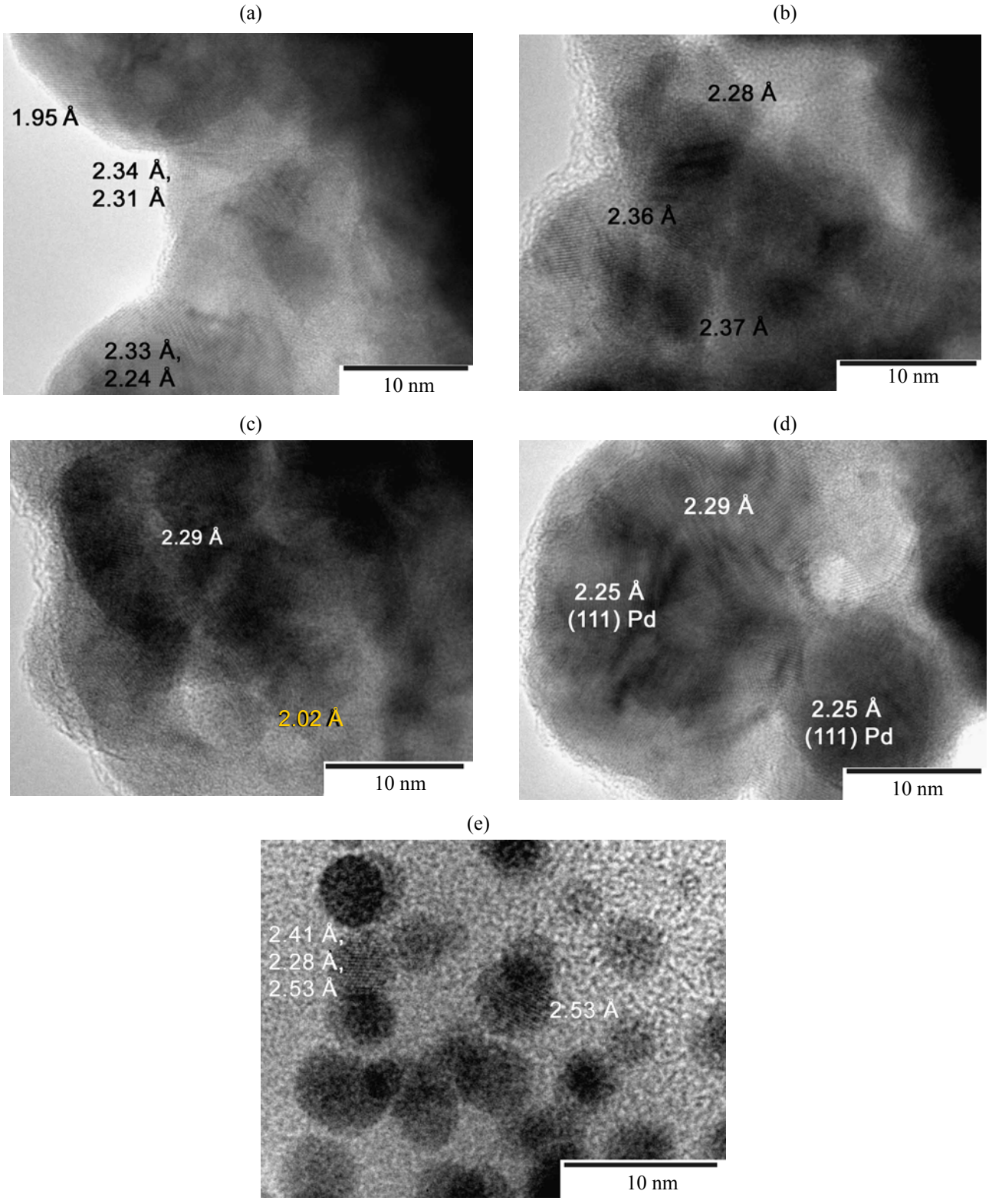

Fig. 2. HRTEM images of a sample isolated under argon from the system $PdCl_2$–0.3 P in DMF. The explanations, see in text.

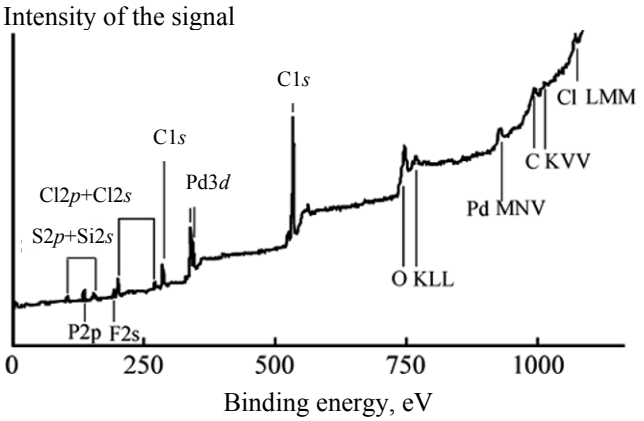

Fig. 3. XPS spectrum of the sample isolated from the system $PdCl_2$–0.3 P in DMF.

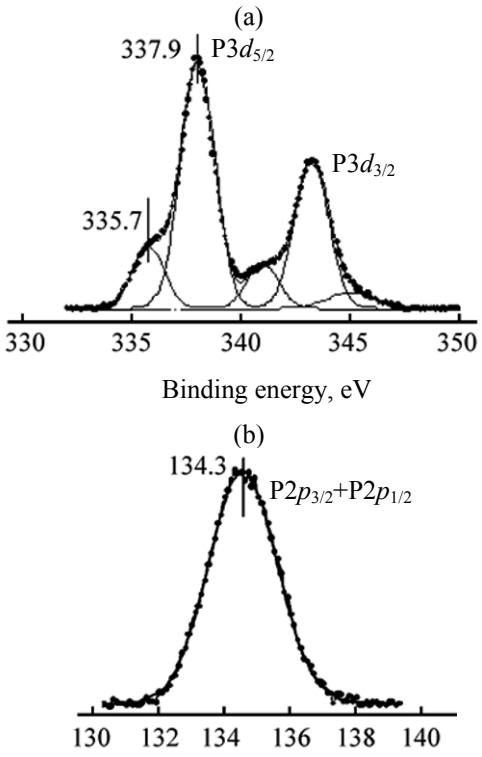

Fig. 4. (a) Pd3*d* and (b) P2*p* spectral lines of the sample isolated from the system $PdCl_2$–0.3 P in DMF.

the sample is indicative of nonuniformity of its composition and the presence of elements Pd, P, O, C, Cl. The observed interplanar distances 2.24, 2.33, 2.34 Å (Fig. 2a), 2.28, 2.37 Å (Fig. 2b) correspond to phosphide $Pd_3P_{0.8}$ (P*nma*) [PDF# 42–0922 (031) 2.2553, (102) 2.3351; (220) 2.2736; (211) 2.3649 Å]. The interplanar distances 2.02 and 2.29 Å are close to those in palladium phosphide $Pd_{15}P_2$ (R3) [PDF# 34-0902 (214) 2.0430, (211) 2.3060 Å] (Fig. 2c); the interplanar distance 2.25 Å (Fig. 2d), to that in palladium nanocrystals (Fm-3m) PDF# 46–1043 (111) 2.2458 Å; the interplanar distances 2.28; 2.41, 2.53 Å (Fig. 2e), to those in $PdCl_2$ (P*nmn*) PDF# 75-0871 (112) 2.2846; (111) 2.4485; (110) 2.5116 Å [12].

The results of HRTEM analysis are consistent with the XRD data and point to the formation of palladium phosphides of different composition as a result of a redox reaction between $PdCl_2$ and P_4 under mild conditions. The observed differences in composition of palladium phosphides most rich in palladium $Pd_{15}P_2$ (HRTEM) and Pd_6P (XRD), in our opinion, are related to the accuracy of determination of interplanar distances in the HRTEM method, and the absence of crystalline palladium in the sample according to XRD can be a result of its high dispersity and low concentration.

We have also studied the surface of the sample using the XPS method. Full spectrum (Fig. 3) is indicative of the presence of a large number of impurities on the surface. In particular, apart from palladium and phosphorus, carbon and oxygen are present. These elements are practically always found in small amounts (no more than 1 at %) even on the surface of pure compounds as a result of adsorption during preparation of the sample for analysis. In our case, the content of carbon and oxygen is large, therefore, it may be assumed that at least carbon was originally present in the sample.

Pd	P	C	O	Cl	Si	P/Pd
4.0	6.2	22	56	6.2	5.8	1.55

Silicon is present on the surface as silicon dioxide. Note that silicon was not detected in the EDXS spectrum when studying by the HRTEM and determination of the elemental composition. Its detection in the XPS spectrum is apparently due to an impurity from the support used for the analysis. Let us consider the state of the elements of the surface layer in more detail.

In the XPS spectrum palladium is characterized by two charge states for which the position of the maxima of the $3d_{5/2}$ component corresponds to the binding energies of 337.9 and 335.7 eV (Fig. 4a). The ground state with the binding energy of 337.9 eV can be assigned to $PdCl_2$ [13], which is consistent with a large amount of chlorine in the sample and with the results of XRD and HRTEM analysis. We believe that the

E_b

second state of palladium with the binding energy of 335.7 eV corresponds to small metal clusters. In particular, for palladium clusters of 1 nm size, the position of the Pd3$d_{5/2}$ level is about 336 eV [14, 15]. The effective positive shift of photoelectron levels of small clusters in comparison with solid palladium metal [BE(Pd3$d_{5/2}$) = 335.2 eV] is connected with less efficient relaxation processes for more disperse systems as a result of smaller zone of conductivity and the valence zone of the metal.

The state of phosphorus in the XPS spectrum is characterized by the P2p line presented in Fig. 4, *b*. The position of the P2p level in the sample is 134.3 eV that corresponds to phosphorus in phosphates, hydrophosphates, and phosphoric acids [16]. The peaks with the binding energies typical for palladium phosphides {BE(Pd3$d_{5/2}$) = 336.2 eV [17]; BE(P2p) = 129–130 eV [18]} are lacking. At first glance, it is reasonable to assume that partial oxidation of palladium phosphides to phosphates occurs on the surface during the preparation of the sample. However, in this case the Pd3d lines corresponding to PdO should appear in the XPS spectrum. The binding energy of the Pd3$d_{5/2}$ level for PdO is 336.7 – 337.0 eV [15]. Besides, it should be mentioned that the surface is strongly enriched with phosphorus. The ratio P/Pd on the surface is 1.55 whereas in the whole sample, according to the data of X-ray microanalysis, it is 0.33. Taking into account that in the redox reaction between $PdCl_2$ and P_4 phosphorous and phosphoric acids are formed, the adsorption of phosphate and/or phosphite anions on the surface of nano-particles is highly probable. The data of XPS on the state of oxygen on the surface of the sample are in compliance with this assumption.

The spectrum of oxygen O1s can be represented as a combination of two lines with the maxima at 532.5 and 533.5 eV (Fig. 5a). The main component with BE(O1s) = 532.5 eV corresponds to the sate of oxygen of the surface hydroxy, hydrocarbonate, and carbonate groups, as well as of phosphoric acids and their salts [19]. Taking into account the results of analysis of the XPS spectra of palladium and phosphorus, we assign this component to the state of oxygen in phosphoric acids. The second component with BE(O1s) = 533.5 eV, whose peak is masked by the intensive peak of oxygen in phosphoric acids, corresponds to the adsorbed water.

Note that the content of both palladium and phosphorus on the surface is rather low. This is due to

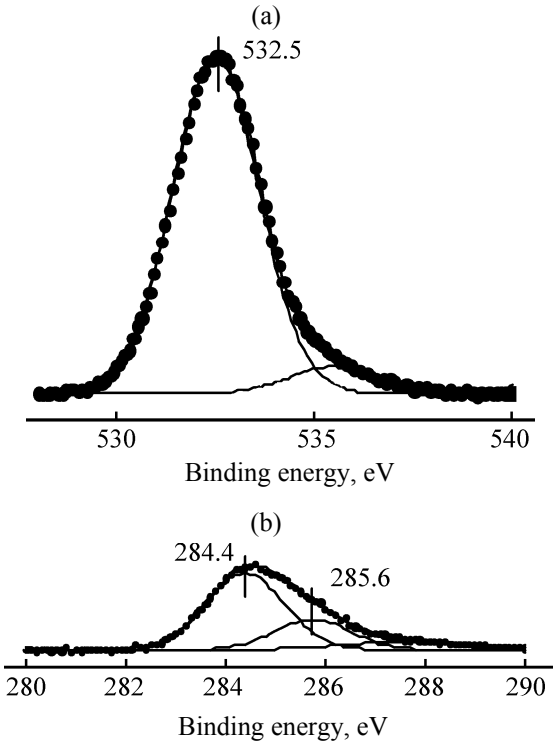

Fig. 5. (a) O1s and (b) C1s spectral lines of the sample isolated from the system $PdCl_2$–0.3 P in DMF.

covering of the surface not only by oxygen- but also carbon-containing compounds. Carbon exists on the surface in the state close to the elemental [BE(C1s) = 284.4 eV] (Fig. 5b). The position of this level corresponds to sp^2-hybridized carbon in graphite, meaning that the surface of the sample is to a large extent represented by organic matrix. The second component in the C1s spectrum at 285.6 eV corresponds to sp^3-hybridized carbon and can be assigned to surface carbon-containing compounds.

Ligand-free clusters are well known to be highly reactive compounds and can react under mild conditions with NH_3 to form surface nitrides, with O_2, to give oxides, etc. [1]. The formation of palladium carbides was observed in the synthesis of palladium nanoparticles at room temperature by the method of sonochemical reduction [20]. The formation of palladium nanoclusters covered with amorphous carbon was observed when complex $Pd_2(dba)_3$ was treated with ultrasound at room temperature [21]. The results of the XPS study suggest that the reaction of $PdCl_2$ with P_4 in DMF under argon is followed not only by the accelerated with HCl hydrolysis of the solvent but also by the decomposition of organic compounds (DMF, C_6H_6) catalyzed with small palladium clusters.

The HRTEM method revealed the presence in the sample of palladium phosphides of different composition, palladium crystallites, and $PdCl_2$. At the same time, the XPS method did not detect palladium or phosphorus on the surface and close-to-surface layers in the states characteristic of metal phosphides. Taking into account the peculiarities of the XPS method, it is reasonable to assume that nanoparticles have the structure of the core–shell type with the core formed by palladium phosphides and the shell by clusters of Pd(0).

Earlier, during chemical simulation of the process of formation of palladium phosphides by the reaction of Pd(0) complex [$Pd(dba)_2$] with white phosphorus under mild conditions we have established that at the first stage the phosphide PdP_2 is formed, whose further reaction with $Pd(dba)_2$ leads to phosphides enriched with palladium [22]. With due regard to these data, the formation of palladium phosphides in the system ($PdCl_2 + P_4$) can be represented as sequential parallel stages.

$$2PdCl_2 + 2P + 6H_2O = 3Pd(0) + 6HCl + 2H_3PO_3,$$
$$2Pd + P_4 = 2PdP_2,$$
$$PdP_2 + 4Pd = Pd_5P_2,$$
$$Pd_5P_2 + Pd = 2Pd_3P,$$
$$Pd_3P + 3Pd = Pd_6P.$$

The reduction of $PdCl_2$ with elemental phosphorus gives rise to formation of Pd(0) atoms, which can aggregate to give small palladium clusters, as well as to react with P_4 to form phosphides Pd_5P_2, Pd_3P, Pd_6P. Analysis of the XPS data leads to the conclusion that in the beginning the second process predominates: the formation of palladium phosphides enriched with palladium. Their further reaction with Pd(0) atoms or small clusters leads to the formation of the core–shell type particles.

Therefore, investigation of the first step of the formation of palladium hydrogenation catalysts modified with elemental phosphorus has shown that the redox reaction of $PdCl_2$ with P_4 in an inert atmosphere under mild conditions results in the formation of palladium phosphides of different composition and small Pd(0) clusters which, apparently, form particles of the core-shell type. The ligand-free Pd(0) clusters, as highly reactive species, not only react with phosphorus, but also catalyze decomposition of organic compounds (DMF, benzene). The formed graphite and anions of phosphoric acids adsorbed on the surface act as stabilizers of nanoparticles.

EXPERIMENTAL

Solvents (benzene, DMF) were purified by standard procedures used at the operation with organometallic compounds [23]. DMF was stored over anhydrous copper sulfate till the formation of green solution for removal of water and admixtures of amines, and then it was distilled in a vacuum (8 mm Hg) at the temperature not exceeding 42°C. Benzene, for deep drying, was distilled over $LiAlH_4$ on a rectification column and kept in an argon atmosphere in sealed ampules over molecular sieves 4A. The concentration of water in benzene determined by the Fischer method [24] was 1.1×10^{-3} M, in DMF – 0.8 M.

White phosphorus, directly before use, was mechanically purified from the surface oxidation products and washed in dry benzene. The solution of white phosphorus in benzene was prepared and kept in an inert atmosphere in a finger-type reactor, equipped with the device for evacuation and filling with argon. ^{31}P NMR: δ_P = –522 ppm. Palladium dichloride of "pure" grade was used without additional purification.

The reaction of $PdCl_2$ with white phosphorus was performed in a finger-type reactor in an inert atmosphere (the ratios of the reagents are given with respect to atomic phosphorus). To the solution of 0.6 mmol of white phosphorus in 2 ml of benzene 0.355 g (2.0 mmol) of $PdCl_2$ in 125 ml of DMF was added at vigorous stirring on a magnetic stirrer. Immediately the color of the solution turned from yellow-orange to deep black. The concentration of hydrochloric acid in DMF was determined by potentiometric titration with KOH solution on a pH-meter pH-410 with glass electrode ESLK-01.7. The nature of the products of phosphorus transformations in solution was analyzed by ^{31}P NMR spectroscopy. After 5 h the solution was evaporated in a vacuum to 1/5 of its volume (40°C, 1 mm Hg) and 10 ml of benzene was added. The formed black precipitate was filtered off, washed thrice with benzene, and dried in a vacuum (30°C, 1 mm Hg). Yield 0.1 g.

On the diffraction curve of the sample the reflexes of crystalline phase are registered belonging to the admixture of the unreacted $PdCl_2$ and a diffuse halo in the range of the reflection angles $2\theta = 35°–45°$. When annealing the sample for conversion into the crystalline state in an inert atmosphere at 400°C for 4 h in a sealed tube a part of the sample was sublimed to give white powder. XRD data for the nonsublimed part of the sample (black powder), *d*/*n*: 2.985, 2.714, 2.562,

2.359, 2.299, 2.254, 2.238, 2.216, 2.121, 2.032, 2.014, 1.907, 1.889, 1.862, 1.845, 1.784, 1.731, 1.569, 1.543, 1.456, 1.409, 1.346, 1.331, 1.290, 1.281 Å (Pd_6P) [12]; 2.738, 2.714, 2.508, 2.439, 2.328, 2.254, 2.216, 2.121, 2.102, 1.997, 1.953, 1.845, 1.731, 1.682, 1.432, 1.378, 1.346, 1.290 Å (Pd_5P_2); 2.693, 2.439, 2.359, 2.254, 2.121, 2.102, 1.997, 1.907, 1.889, 1.862, 1.802, 1.682, 1.615, 1.511, 1.378, 1.331, 1.310, 1.290 Å (Pd_3P) [25]. XRD data for the sublimed part of the sample (white powder), *d*/*n*: 3.875, 3.745, 2.237, 1.938, 1.736, 1.583, 1.370, 1.290, 1.226 (NH_4Cl) [12]. Lines 2.778, 2.585, 1.579 were not identified.

The XRD analysis was performed on a DRON-3M difractometer with CuK_α radiation.

HRTEM studies were performed on an electron microscope JEM-2010, accelerating voltage 200 with lattice resolution limit of 0.14 nm. The images were recorded with the use of CCD camera. The sample was dispersed on a copper support from the suspension in hexane using an ultrasound dispergator. The local analysis of the elemental composition was performed on an energy dispersive spectrometer EDAX Phoenix with Si(Li) detector and resolution in energy of ca. 130 eV. Parameters of the particle images on the pictures were measured using iTEM 5.0 and Digital Micrographs 3.3.1 programs. For analysis of periodic structures and filtration of the images the Fourier methods FFT and IFFT were used. To determine the interlayer distances, the profiles of intensity of the images obtained by the DigitalMicrographs 3.3.1 program, were used.

The surface of the sample was investigated on a photoelectron spectrometer KRATOS ES 300. Before placing into spectrometer, the sample was ground in an agate mortar and placed on a conductive carbon tape. XPS spectra were registered after a vacuum of 1×10^{-8} Torr was reached. To analyze the qualitative composition of the surface and to determine admixtures, the total spectum in the range 0–1100 eV was obtained with the step in energy of 1 eV with the transmission energy of the analyzer HV = 50 eV. To analyze the quantitative composition of the surface and charge states of the elements, the precision specta of separate photoelectron lines were obtained with the step in energy of 0.1 eV with the transmission energy of the analyzer HV = 25 eV. The analyzer was calibrated using the lines of metal gold and copper Au*f*4 и Cu2*p* at 84.0 and 932.7 eV, respectively. The spectra were calibrated using the C1*s* line, whose binding energy was taken to be 285.1 eV. As a primary radiation, the K_α-magnesium line was used ($h\nu$ = 1253.6 eV).

ACKNOWLEDGMENTS

The authors are grateful to R.V. Gulyaev and A.V. Ishchenko for the assistance in XPS and HRTEM studies.

This work was performed under the Federal Targeted Program "Scientific and pedagogical staff of innovative Russia" (grant 14.B37.21.0795) and with financial support from Irkutsk State University (grant 2011-04-04).

REFERENCES

1. Pomogailo, A.D., Rozenberg, A.S., and Ufland, I.E., *Nanochastitsy metallov v polimerakh* (Metal Nanoparticles in Polymers), Moscow: Khimiya, 2000.
2. Suzdalev, I.P., *Nanotekhnologiya: Fiziko-khimiya nanoklasterov, nanostruktur i nanomaterialov* (Nanotechnology: Physical Chemistry of Nanoclusters, Nanostructures, and Nanomaterials), Moscow: Knizhnyi Dom "LIBROKOM," 2009.
3. Mansoori, G.A., *Principles of Nanotechnology : Molecular-Based Study Of Condensed Matter In Small Systems*, World Sci. Publ. Co., 2005.
4. Ott, L.S. and Finke, R.G., *Coord. Chem. Rev*., 2007, vol. 251, nos. 9–10, p. 1075.
5. Durand, J., Teuma, E., and Gomez ,M., *Eur. J. Inorg. Chem*., 2008, no. 23, p. 3577.
6. Moiseev, I.I. and Vargaftik, M.N., *Russ. J. Gen. Chem. Engl. Transl*., 2002, vol. 72, no. 4, p. 512.
7. Belykh, L.B., Titova, Yu.Yu., Umanets, V.A., Rokhin, A.V., and Schmidt, F.K., A*ppl. Cat. (A),* 2011, vol. 401, p. 65.
8. Skripov, N.I., Belykh, L.B., Belonogova, L.N., Umanets, V.A., Ryzhkovich, E.N., and Schmidt, F.K., *Kinet. Catal.,* 2010, vol. 51, no. 5, p. 714.
9. Schmidt, F.K., Belykh, L.B., and Goremyka, T.V., *Kinet. Catal*., 2003, vol. 44, no. 5, p. 623.
10. Belykh, L.B., Skripov, N.I., Belonogova, L.N., Umanets, V.A., and Schmidt, F.K., *Kinet. Catal*., 2010, vol. 51, no. 1, p. 42.
11. Belykh, L.B., Skripov, N.I., Belonogova, L.N., Umanets, V.A., Stepanova, T.P., and Schmidt, F.K., *Kinet. Catal*., 2011, vol. 52, no. 5, p. 702.
12. *Powder Diffraction File. Q. Hanawalt Search Manual Inorganic Phases*, JCPDS, 1992, pp. 1–42.
13. Gopinath, R., Lingaiah, N., Sreedhar, B., Suryanarayana, I., Sai Prasad, P.S., and Obuchi, A., A*ppl. Catal. (B),* 2003, vol. 46, no. 3, p. 587.
14. Wertheim, G.K., *Zeitschrift fur Physik (D)*, 1989, vol. 12, nos. 1–4, p. 319.

15. Tsyrul'nikov, P.G., Afonasenko, T.N., Koshcheev, S.V., and Boronin, A.I., *Kinet. Catal*., 2007, vol. 48, no. 5, p. 728.
16. Le Bloa, A., Hbib, H., Bonnaud, O., Meinel, J., and Quemerais, A., *Rev. Phys.* A*ppl*., 1989, vol. 24, p. 545.
17. *Successful Design of Catalysts*, Inui, T., Ed., Amsterdam: Elsevier Science Publishers B.V., 1988, p. 3.
18. Nemoshkalenko, V.V., Didyk, V.V., Krivitskii, V.P., and Senkevich, A.I., *Zh. Neorg. Khim*., 1983, vol. 28, no. 9, p. 2182.
19. Sherwood P.M.A., *Surface Science Spectra*, 2002, vol. 9, p. 62.
20. Okitsu, K., Mizukoshi, Y., Bandow, H., Yamamoto, T.A., Nagata, Y., and Maeda, Y., *J. Phys. Chem. (B)*, 1997, vol. 101, p. 5470.
21. Arul Dhas, N., Cohen, H., and Gedanken, A., *J. Phys. Chem. (B)*, 1997, vol. 101, p. 6834.
22. Skripov, N.I., Belykh, L.B., Belonogova, L.N., Rokhin, A.V., Stepanova, T.P., and Shmidt, F.K., *Russ. J. Gen. Chem. Engl. Transl*., 2012, vol. 82, no. 2, p. 206.
23. Gordon, A.J. and Ford, R.A., *The Chemist's Companion*, New York: Wiley, 1972.
24. Mitchell, J. and Smith, D.M., *Aquametry*, New York: Wiley, 1977.
25. Boone, S. and Kleppa, O.J., *J. Chem. Thermodynamics*, 1991, vol. 23, p. 1147.